Journal of Hydrology 609 (2022) 127694

Contents lists available at ScienceDirect

Journal of Hydrology

journal homepage: www.elsevier.com/locate/jhydrol

Research papers

Impact of dam construction on the spawning grounds of the four major Chinese carps in the Three Gorges Reservoir

Caihong Tang, Qiming Yan, Wenda Li, Xiyan Yang, Shanghong Zhang *

School of Water Resources and Hydropower Engineering, North China Electric Power University, Beijing 102206, China

ARTICLE INFO

This manuscript was handled by Nandita Basu, Editor-in-Chief, with the assistance of Andrea E. Brookfield, Associate Editor

Keywords:
Four major Chinese carps
Three Gorges Reservoir
Spawning grounds
Hydrodynamic model

ABSTRACT

The construction of dams has tremendously altered the water flow and environmental conditions of natural rivers, severely affecting the habitat and reproduction activities of aquatic organisms. In this study, we constructed a reproduction suitability model for the four major Chinese carps (FMCCs) in the upper reaches of the Yangtze River and related this to a one-dimensional hydrodynamic model of the Three Gorges Reservoir (TGR). Stochastic flood modelling was used to simulate a series of river floods before and after construction of the Three Gorges Dam (TGD). The simulated floods were used as the input boundaries of the hydrodynamic model to then simulate complex flow conditions in the upper reaches of the Yangtze River before and after dam construction, so as to simulate the spatial distribution and changes in the spawning grounds of the FMCCs. We found that the reproduction suitability for the FMCCs in the TGR decreased during the post-dam period, and most of the spawning grounds moved to the river reach above Zhongxian. The FMCCs were found to initially have a total of nine spawning grounds, but during the post-dam period there were six spawning grounds likely in the 60-km stretch of Zhutuo–Jiangjin section and in the 255-km stretch of Banan–Zhongxian section. By setting four different water levels in front of the dam (corresponding to no-dam, low-dam, middle-dam, and high-dam scenarios), we examined the effects of dam sizes on the spatial distribution of the FMCCs' spawning grounds. The results showed that the area of affected spawning grounds positively correlated with the dam's size, with high-dam scenario (corresponding to the construction of the TGD) being especially impactful through a net loss of spawning grounds extending 101 km upstream from the dam. The results of this study offer scientific guidance for the ecological regulation of the TGR.

1. Introduction

Dam construction impacts both of river ecology and human society. The construction of dams not only alters the original runoff and sediment transport of rivers, but also profoundly affects the resident aquatic organisms. Dams block the migration of fish and other aquatic organisms, and affect water regime elements such as river flow velocity, water levels, and water temperatures during reservoir operation (Corbacho and Sanchez, 2001; Morita and Yamamoto, 2002; Santos et al., 2006; MacDougall et al., 2007). These alterations, in turn, affect the spawning and survival of aquatic organisms. Understanding these impacts may benefit the entire river ecosystem by guiding macro-level ecological regulations that attempt to balance the relationship between social development and ecological protection.

The four major Chinese carps (FMCCs)—namely, black carp (*Mylopharyngodon piceus*), grass carp (*Ctenopharyngodon idella*), silver carp (*Hypophthalmichthys molitrix*), and bighead carp (*H. nobilis*)—are important economic fishes in China and are widely distributed in the Yangtze River basin. The Yangtze River has become an important breeding ground and habitat for the FMCCs. A survey by Yi et al. (1988) identified 30 spawning sites used by the FMCCs in the main stream of the river prior to construction of the Three Gorges Dam (TGD). In particular, the river sections above Yichang spanned 29.6% of the total area and contained 11 spawning sites (at Chongqing, Mudong, Changshou, Fuling, Gaojiazhen, Zhongxian, Wanzhou, Yunyang, Wushan, Zigui, and Sandouping) (Yi et al., 1988). However, aquatic ecosystems are vulnerable to interference from various human activities (Wang et al., 2020). The impoundment of the TGD in 2003 blocked the natural river course, preventing fish migration. This has hindered fish reproduction, triggering a steep decline in the spawning volume of the FMCCs, as the cross-sectional shape of the river channel, hydrological processes, water temperature regimes, and water quality conditions have undergone

* Corresponding author.
E-mail address: zhangsh928@126.com (S. Zhang).

https://doi.org/10.1016/j.jhydrol.2022.127694
Received 19 July 2021; Received in revised form 25 February 2022; Accepted 3 March 2022
Available online 8 March 2022

major changes since the dam was built (Galat and Lipkin, 2000; Lytle and Poff, 2004; Liu et al., 2018). Because of these changes, the eggs of the FMCCs must drift for a longer time to complete hatching, and the locations of the spawning grounds have gradually shifted toward the upper reaches of the Yangtze River (Jiang et al., 2010). Therefore, research on the FMCCs' spawning grounds is urgently needed (Jiang et al., 2010; Liu et al., 2018). Not only will it help to clarify the impact of the dam's construction on the spawning behavior of the FMCCs in the upper reaches of the Yangtze River, but it will also further expand our understanding of the serious ecological threat to the river following construction of the dam.

Numerous researchers have expressed concern about the breeding and habitat conditions of the FMCCs in the Three Gorges Reservoir (TGR) during the post-dam period (Li et al., 2008; Jiang et al., 2010; Wang et al., 2020; Yang et al., 2021). Li et al. (2008) suggested that construction of the TGD would lead to a decline in the number of spawning ground available for the FMCCs in the reservoir area. However, throughout the natural evolution of hydrological and hydrodynamic conditions, the FMCCs have actively spawned in some river reaches of the reservoir, and spawning has increased since 2008. Although the proportion of the FMCCs' broodstock is usually less than 4% of the catch in a given year, the proportion of the annual catch by weight exceeds 10% (Yang et al., 2017). This indicates that the reservoir area still provides suitable spawning grounds and habitat for adults of the FMCCs. Previous studies reported that in the post-dam period the FMCCs more often spawn in the river reach above Zhongxian than in the lower reach, and that important spawning grounds have been established at the downstream end of the TGR (Mu et al., 2014; Wang et al, 2015; Li et al., 2020; Mu, 2014).

Numerous studies have explored the impact of the TGD on the spawning activities of the FMCCs, especially in waters downstream of the dam. Yu et al. (2019) found that large-scale cascade reservoirs had changed the frequency distribution of flow, sediment, and water temperature, and these changes affect the spawning of the FMCCs below the TGR. Upstream reservoir releases significantly changed the water temperature of the downstream river, which has resulted in a spawning delay of 4–5 weeks for the FMCCs spawning (Wang et al., 2020). Ban et al. (2019) used the range of variation method with selected hydrological indicators to examine the impacts of changes of hydrological variability on spawning by the FMCCs downstream of the TGR; they found that the high-pulse duration, rate of increased inflow, and rise in the water level are key factors affecting spawning success. Wang et al. (2014b) asserted that the TGD changed the thermal state of the discharge water below the dam, which has led to delayed spawning by the FMCCs. Liu et al. (2018) established a two-dimensional hydrodynamic model of the downstream reach to determine the correlation between vorticity in the spawning grounds and the distribution of the FMCCs. In addition, Wang et al. (2014a) used a genetic programming calculation to quantitatively uncover (linearly or nonlinearly) the impact of various hydrological indicators on the spawning behavior of the FMCCs during the pre- and post-dam periods, taking into account the decrease in water temperature when the water flow increases.

The above-mentioned studies focused on the impact of the dam's construction on the spawning activities of the FMCCs. Though some studies comprehensively simulated the indices affecting the FMCCs' spawning activities as a whole system, they used only measured flood simulations or steady-state simulations (i.e., constant flood conditions such as 10,000 m^3/s, 20,000 m^3/s, and so on). Few studies have considered the impacts of time-variable inflow hydrographs. Additionally, previous studies on changes in spawning ground locations during the pre- and post-dam periods tended to focus on a single spawning ground and failed to assess changes in the spatial extent of spawning grounds in the TGR. There is also a lack of relevant quantitative research on the general distribution of fish spawning sites relative to dams. More importantly, because the flow conditions are significantly altered in dammed rivers, quantitative research is needed on the extent of the impact of dams on river flow conditions. For instance, traditional steady-state flood simulations would hardly reflect the response of the FMCCs to changes in flow conditions caused by different inflow hydrographs. Moreover, the simulation of one specific or several measured flood processes usually would not accurately predict the entire spatial distribution of the spawning grounds. Instead, simulation of a large number of stochastic flood events in the reservoir area would effectively increase the number of simulated samples and thereby reliably reflect changes to the spatial distribution of spawning grounds under complex inflows. With a large number of simulations, it is also possible to further explore the impact of dams on the hydrodynamic processes in the reservoir area, which is unattainable with traditional simulations of constant flood flow rates. Therefore, stochastic flood modelling can be indispensable to studying the habitat and reproduction suitability for aquatic organisms in dammed rivers.

This study addressed these knowledge gaps by investigating the reproductive suitability of the FMCCs in different river reaches of the TGD reservoir area. A two-step method was applied. (1) To determine changes in the spatial distribution of the spawning grounds of the FMCCs in the upper reaches of the Yangtze River (specially between Zhutuo and the TGD) in the pre- and post-dam periods, complex inflow scenarios were simulated based on a model of FMCCs reproduction suitability in the TGR. (2) To analyze the impact of different dam scenarios on the locations and extent of spawning grounds of the FMCCs, different dam sizes (defined as the water level immediately in front of the dam) were further assumed and simulations were carried out.

2. Study area

The TGR is a narrow river-type reservoir, and in the dry season its backwater area extends from the dam site to Chongqing (Fig. 1). However, the discharge process of the TGR showed large differences based on the inflow hydrographs of Cuntan and Zhutuo stations, respectively (Zhang et al., 2017). Thus Zhutuo station was regarded as the upstream boundary to calculate the water discharge, incoming runoff, reservoir capacity, and sediment load of the TGR (Zhang et al., 2017; Ren et al., 2021). Hence, this study considered the 756-km stretch between Zhutuo and the dam site as the study area (Fig. 1). Owing to the complex vertical composition of the water body and the suitable flow conditions, this section of the river now constitutes an important aquatic ecosystem in China. Many small bays once existed on both sides of the river channel, in which aquatic plants and plankton inhabited, and the bays provided natural shelter as well as nutrients for resident aquatic organisms. Changes in water flow and water temperature provided suitable habitat and spawning conditions for the FMCCs. Following the construction of the TGD, the water level in the reservoir area rose, and the original water flow conditions and regional climate changed dramatically. The spatial distribution of spawning grounds in the TGR also underwent tremendous changes. To assess the impact of the dam on the spatial distribution of the FMCCs' spawning grounds, we allocated 394 cross-sections of the TGR into 14 river sections that are potential spawning grounds, based on the topography and distribution of spawning grounds in the pre-dam period (Fig. 1, Table 1).

3. Methods

3.1. Research approach

The TGR (between Zhutuo and the TGD) was selected as the study area. A hydrodynamic model was established and validated with measured data, using MIKE 11 software developed by DHI. A large number of floods based on a stochastic model were generated as the input boundaries of the hydrodynamic model intended to simulate the flood evolution process during the pre- and post-dam periods. The habitat suitability index (HSI) was used to describe habitat suitability for the FMCCs in different sections of the TGR. The specific research steps

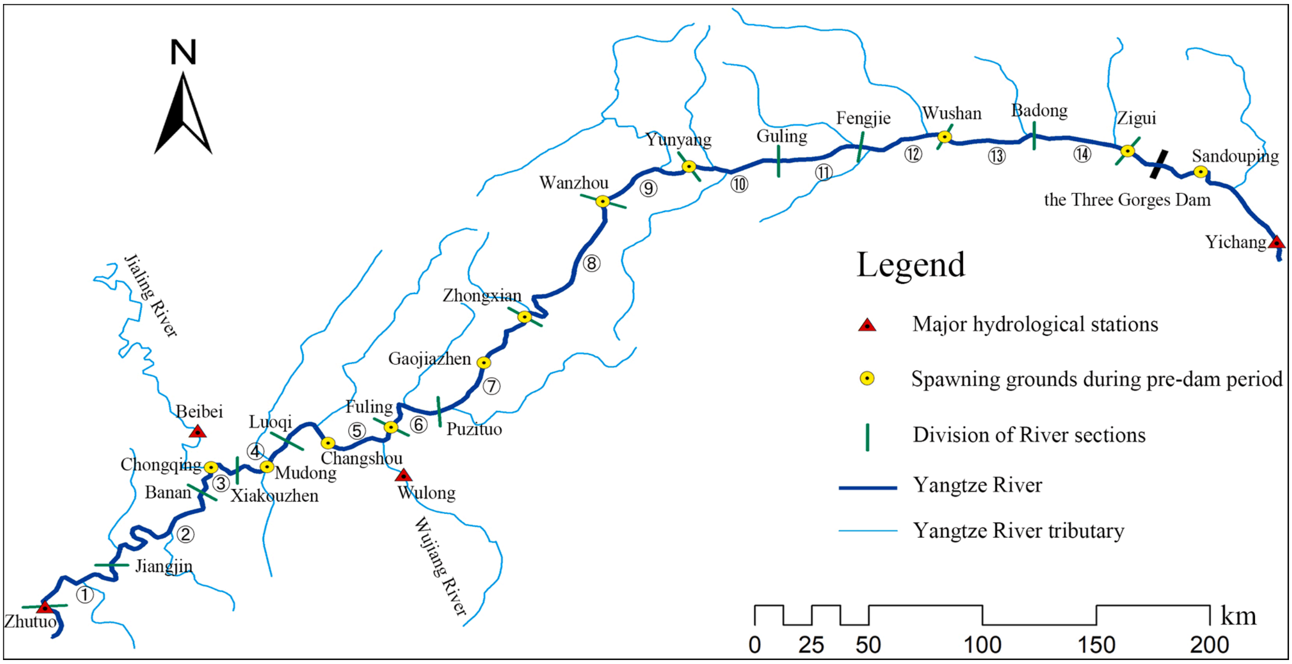

Fig. 1. Map of the Three Gorges Reservoir and locations of spawning grounds of the four major Chinese carps before construction of the Three Gorges Dam. The numbers correspond to the designated river sections listed in Table 1.

Table 1
Designated sections of the Three Gorges Reservoir.

Serial number	River section name	Starting and ending position of cross-section (km)		Number of cross-sections	Length of each river section (km)
X1	Zhutuo–Jiangjin	0	60	28	60
X2	Jiangjin–Banan	60	131	34	71
X3	Banan–Xiakouzhen	131	159	25	28
X4	Xiakouzhen–Luoqi	159	211	17	52
X5	Luoqi–Fuling	211	274	34	63
X6	Fuling–Puzituo	274	315	26	41
X7	Puzituo–Zhongxian	315	386	38	71
X8	Zhongxian–Wanzhou	386	465	41	79
X9	Wanzhou–Yunyang	465	519	24	54
X10	Yunyang–Guling	519	552	17	33
X11	Guling–Fengjie	552	590	18	38
X12	Fengjie–Wushan	590	632	21	42
X13	Wushan–Badong	632	686	28	54
X14	Badong–TGD	686	756	43	70

were as follows:

(1) Based on the HSI method, the key indices affecting the reproduction activities of the FMCCs in the Yangtze River were selected, and a habitat suitability evaluation system for the FMCCs in the upper reaches of the Yangtze River was constructed.
(2) MIKE 11 software was used to establish a one-dimensional hydrodynamic model of the TGR. Based on the available statistics and stochastic hydrology, a periodic stationary autoregressive model of daily flow was constructed to generate a large number of potential flood processes. Thereafter, the progression of a large number of stochastic inflow floods was simulated to obtain changes in the hydrological index. Combining the simulation results for water temperature, we evaluated the reproductive suitability of the FMCCs in the reservoir area under complex inflow scenarios to determine the spatial distribution of the spawning grounds.
(3) Based on the flow conditions during the pre- and post-dam periods, the spatial distribution of the spawning grounds of the FMCCs in the river reach between Zhutuo to the TGD was analyzed, and the impact of different dam scenarios on the spawning grounds of the FMCCs was further investigated. The overall research approach is depicted by the flow chart in Fig. 2.

3.2. Reproduction suitability curves for the four major Chinese carps

The HSI is a classic method for quantitatively describing habitat suitability (Brown et al., 2000). It can be used to characterize the response of organisms to various environmental factors in the surrounding habitat (Cho et al., 2012; Knudson et al., 2015). The FMCCs produce eggs in response to changes in water flow conditions and the environmental factors in specific river sections, and these river sections become suitable spawning grounds. In this study, three important indices that can trigger the spawning behavior of the FMCCs (i.e., flow velocity, water temperature, and water level fluctuation) were selected to determine the HSI, and a model of FMCCs' reproduction suitability was constructed to locate the spawning grounds in the TGR.

3.2.1. Water flow velocity

The FMCCs are pelagic river spawners with drifting, semi-buoyant eggs that must remain in suspension in the water column until hatching. The newly produced eggs have a water-swelling density slightly greater than that of water and require a certain flow rate to hatch (Yi et al., 2010). While drifting down the river, the fertilized eggs hatch into juveniles. A flow velocity of 0.25–0.9 m/s can provide suitable spawning conditions by the FMCCs; the eggs of these carps begin to sink when the flow velocity is less than 0.27 m/s; most of the eggs will fall on the riverbed at a velocity of less than 0.25 m/s, and all eggs will sink at a velocity of less than 0.1 m/s (Cao et al., 1987; Yi and Le, 2011). Some studies have shown that only a portion of the eggs can hatch out if they settle on the riverbed (Garcia et al., 2015; Prada et al., 2018). This study assumed that the drifting fluvial eggs would die outside the suitable flow velocity ranges, to be determined by the hydrodynamic model in this study.

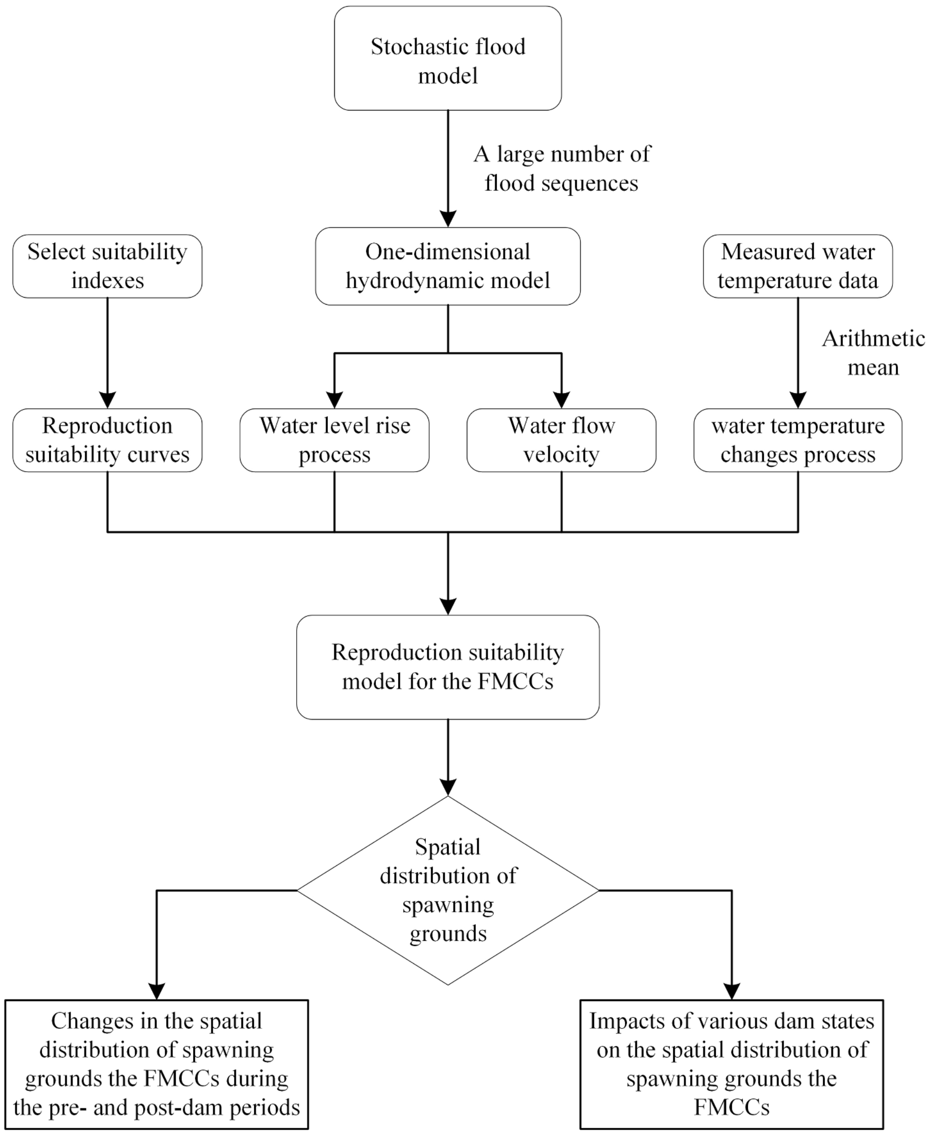

Fig. 2. Flow chart of the research approach. FMCCs: four major Chinese carps (namely, *Mylopharyngodon piceus*, *Ctenopharyngodon idella*, *Hypophthalmichthys molitrix*, and *H. nobilis*).

3.2.2. Water temperature

Water temperatures in the TGR from late April to late July each year are suitable for the FMCCs to spawn and reproduce. During this time, the main stream of the Yangtze River generally fluctuates between 18 °C and 28 °C. The FMCCs in the Yangtze River do not breed at temperatures below 18 °C. Since the completion of the TGD, the reproduction time of the FMCCs has been gradually delayed (Wang et al., 2020). The peak spawning period is at water temperatures of 21–24 °C (Yi et al., 1988), which occurs from May to June (Chen and Li, 2015); so long as the river water temperatures are above the lower temperature threshold of 18 °C (Wang et al., 2008), the FMCCs can spawn.

3.2.3. Water level fluctuation

Water level fluctuation is an important index influencing the spawning activities of the FMCCs. Provided that the water temperature and flow velocity are suitable, the mature broodstock requires an increase in water flow to exhibit spawning behavior (Yi et al., 2010). In most cases, the spawning activities of the FMCCs are carried out during a period of rising water; when the water level drops and the flow rate slows, the spawning activities tend to stop. The FMCCs can be induced to spawn when the water level rises continuously for 4–5 days (Wang et al., 2008; Yi et al., 2010) and when high water levels are maintained for 2.5 days (Wang and Gao, 2017).

In summary, the spawning activities of the FMCCs in the Yangtze River are affected by many factors; thus, it would be impossible to accurately simulate the spawning situation in a certain section of the river by considering only isolated factors. A model of FMCCs reproduction suitability was established based on the averaged water temperature from 1 May to 10 June at seven stations (i.e., Zhutuo, Tongguanyi, Cuntan, Qingxichang, Wanzhou, Guandukou, and Nanjinguan) in both the pre- and post-dam periods, because various indices reveal that conditions in this period are suitable for the FMCCs to spawn. According to the response degree of the FMCCs to the changes in different indices, the reproduction suitability curves to the changes in water flow velocity, water temperature, and daily average water level fluctuation were obtained (Fig. 3). The data applied to the reproduction suitability curves were based on expert suggestions and references to the literature (Ban et al., 2009). The formula for calculating HSI was based on the geometric average method (Yi et al., 2010):

$$HSI = (I_V I_T I_{dz})^{\frac{1}{3}} \quad (1)$$

where the value of HSI ranging from 0 to 1; and I_V, I_T, and I_{dz} represent

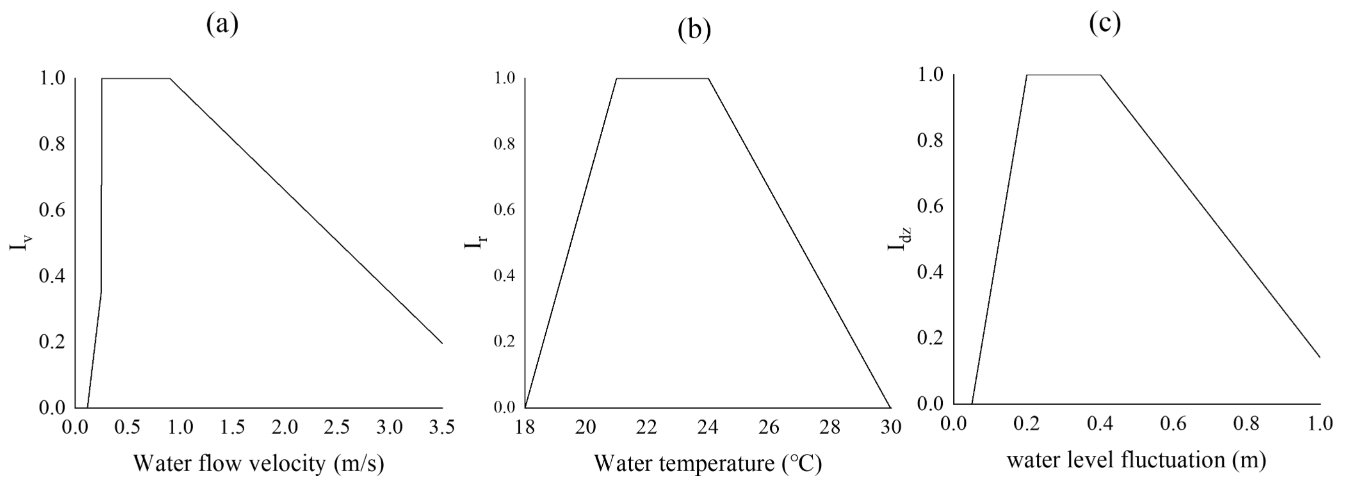

Fig. 3. Reproduction suitability curves for the four major Chinese carps in the Yangtze River.

the water flow velocity index, water temperature index, and water level fluctuation index, respectively, with values that likewise range between 0 and 1.

The determinations of mean velocities and water level fluctuations came from the one-dimensional hydrodynamic model (described below). Finally, the HSI values of each river cross-section along the reservoir area were calculated based on the FMCCs' reproduction suitability model. Considering suitability based on different values of HSI (Jiang et al., 2019) (Table 2), the reservoir locations of cross-sections suitable for spawning of the FMCCs could then be evaluated.

Owing to discontinuous conditions across each channel cross-section, the distribution of HSI values at different positions in the channel was relatively scattered. This study divided the reservoir area into multiple river sections, as listed in Table 1. To clearly describe the habitat suitability of the sections for the FMCCs, we defined a suitability proportion, *W*, which represents the proportion of the number of cross-sections having HSI values greater than 0.5 among the total number of sections in the study area. Moreover, *W* could represent the scale of the spawning grounds within a given river section, as well as the possibility that a river section would become a spawning ground for the FMCCs under stochastic flood conditions. A higher *W* value indicates proportionately greater suitability for the FMCCs, meaning the more likely the river section is to become a spawning ground. The formula is:

$$W = \frac{n}{N} \times 100\% \tag{2}$$

where *n* represents the number of cross-sections with HSI greater than 0.5 in a given river section; *N* represents the total number of cross-sections in this river section; and *W* represents the proportion of suitable area (that is, the overall suitability in a certain river section of the FMCCs). The range of the values of *W* is 0–1.

3.3. Hydrodynamic model of the Three Gorges Reservoir

3.3.1. Stochastic inflow floods

The spatial distribution of the FMCCs' spawning grounds under one or several actual flood simulations is often subject to uncertainty because of various influencing factors each year. Stochastic flood simulation can generate a large number of flood sequences and predict future water regimes based on statistical and actual hydrological data (Gharari and Razavi, 2018). Our study established a stochastic flood model to simulate changes in water flow conditions under complex inflows, to evaluate changes in the spatial distributions of the FMCCs' spawning grounds. In this study, we established a periodic stationary autoregressive model of daily flow in the TGR to realize the stochastic simulation of the flood process at three main inflow stations— (Zhutuo, Beibei, and Wulong)— referenced from Jing et al. (2020). This model divided a year into several periods based on the consistency of changes in the autocorrelation structure of the daily flow, and it established a corresponding stationary autoregressive model for each period. The model used the measured daily flow data of the main inflow stations from 1957 to 2016 (60 years, with 28 days in February each year) as the modeling data. According to the statistical characteristics of the daily flow data and the differences in autocorrelation coefficients in different periods, combined with the principle of staging, the annual daily flow process was specifically divided into *r* periods. The periodic stationary autoregressive model of daily flow was expressed according to the formula:

$$Z_t = \begin{cases} \sum_{i=1}^{P_1} \varphi_i^1 Z_{t-i} + \varepsilon_t^1 & 1 \le t \le T_1 \\ \sum_{i=1}^{P_2} \varphi_i^2 Z_{t-i} + \varepsilon_t^2 & T_1 < t \le T_2 \\ \cdots\cdots & \\ \sum_{i=1}^{P_r} \varphi_i^r Z_{t-i} + \varepsilon_t^r & T_{r-1} < t \le 365 \end{cases} \tag{3}$$

where Z_t is the flow simulation sequence of day *t*, which is standardized and normalized; T_d ($d = 1, 2, \ldots, r$-1) is the start day of the different periods, and *r* is the number of periods; $\varphi_1^j, \varphi_2^j, \ldots, \varphi_{P_j}^j$ is the autoregressive coefficient of the period *j*; P_j is the level of the period ($j = 1, 2, \ldots, r$); and ε_t^j is the normal independent stochastic variable (mean value is 0, square error is ${\sigma_\varepsilon^j}^2$). The autoregressive coefficients were estimated using the Yule–Walker equations as follows:

$$\begin{bmatrix} \varphi_1^j \\ \varphi_2^j \\ \vdots \\ \varphi_{P_j}^j \end{bmatrix} = \begin{bmatrix} 1 & \rho_1^j & \rho_2^j & \cdots & \rho_{P_j-1}^j \\ \rho_1^j & 1 & \rho_1^j & \cdots & \rho_{P_j-2}^j \\ \vdots & \vdots & \vdots & \cdots & \vdots \\ \rho_{P_j-1}^j & \rho_{P_j-2}^j & \rho_{P_j-3}^j & \cdots & 1 \end{bmatrix} \begin{bmatrix} \rho_1^j \\ \rho_2^j \\ \vdots \\ \rho_{P_j}^j \end{bmatrix} \tag{4}$$

where $\rho_1^j, \rho_2^j, \ldots, \rho_{P_j}^j$ is an average value of the autocorrelation co-

Table 2
Habitat Suitability Index (HSI) values for the four major Chinese carps in the Three Gorges Reservoir.

HSI	Suitability
0–0.5	Poor
0.5–0.8	Generally suitable
0.8–1	Suitable

efficients $\gamma_{i,j}$ of level 1, 2, …, P_j in different periods. The residual variance ${\sigma_\varepsilon^j}^2$ was calculated using the formula:

$$ {\sigma_\varepsilon^j}^2 = 1 - \varphi_1^j \rho_1^j - \varphi_2^j \rho_2^j - \cdots - \varphi_{P_j}^j \rho_{P_j}^j \tag{5} $$

According to the generated stochastic flood process of the main inflow stations, 2000 inflow scenarios at the Zhutuo, Wulong, and Beibei hydrological stations were formed.

3.3.2. Simulation of three indices

MIKE 11 was used to build a one-dimensional hydrodynamic model to simulate the evolution of different flood processes. This model was based on the Saint-Venant equations and solved using the Abbott–Ionescu format. The governing equations are as follows. More model details can be found in Yan et al. (2021).

The continuity equation is:

$$ B\frac{\partial Z}{\partial t} + \frac{\partial Q}{\partial x} = q \tag{6} $$

and the momentum equation is:

$$ \frac{\partial Q}{\partial t} + \frac{\partial}{\partial x}\left(\frac{Q^2}{A}\right) + gA\left(\frac{\partial Z}{\partial x} + \frac{Q|Q|}{K^2}\right) = 0 \tag{7} $$

where x is the distance along the river in meters (m); t is time in second (s); Z (m) and Q (m^3/s) are the water level and flow through a river section at any time; A (m^2) is the cross-section area; q (m^2/s) is the lateral inflow per unit length; B (m) is the water width of the river section; g (m/s^2) is gravitational acceleration, and K (m^3/s) is the flow modulus.

To reflect as much as possible the influence of the different forms of all stochastic flood processes and the statistical laws on the simulation results, we selected 2000 flood processes as the inflow conditions of the one-dimensional hydrodynamic model. This sample size of 2000 is representative of the water flow patterns of most possible flood processes and can generate the flood evolution under complex inflow conditions. The one-dimensional hydrodynamic model simulated the changes in water level and water velocity throughout the study reach in various periods, which provided relevant data support for the evaluation of FMCCs reproduction suitability. The channel shapes were generalized from the 414 measured cross-section data in 2012, provided by Changjiang Water Resources Commission of the Ministry of Water Resources, China, and the initial water surface elevation was calculated by the hydrodynamic model under different inflow conditions. Thereafter, the one-dimensional hydrodynamic model was used to simulate each flood using the pre- and post-dam conditions. During the pre-dam period, the water level–water discharge relationship curve of Yichang station was fit under natural flow conditions based on the measured data from 1990 to 2003, to be used as the outflow boundary condition for the model. During the post-dam period, the model calculation used the water level change regime of the TGR from 1 May to 10 June as the downstream boundary condition (Li et al., 2018); that is, the starting water level was 155 m, dropping to 145 m.

Daily average water temperatures in the pre- and post-dam periods were calculated based on the daily measured data at seven stations in the Zhutuo–TGD section. The formula is as follows:

$$ T_i = \frac{\sum_{j=1}^{n} T_{j,i}}{n} \tag{8} $$

where T_i ($i = 1, 2, 3, \ldots, n$) is the water temperature on the i_{th} day in the simulated water temperature; $T_{j,i}$ ($j = 1, 2, 3, \ldots, n$; $i = 1, 2, 3, \ldots, n$) is the water temperature value of the i_{th} day in the j_{th} year in the actual measured water temperature.

Thereafter, this study took the daily water temperature calculation results from 1 May to 10 June as the daily water temperature state under stochastic flood conditions. The water temperature data came from the actual daily average water temperature data of seven hydrological stations for the pre-dam period (1994–2002) and post-dam period (2003–2017). Finally, the flow velocity and water level fluctuation of each flood process were calculated and combined with the changes of water temperature to form the basic calculation data of the FMCCs' reproduction suitability model.

3.4. Reproduction suitability model of the four major Chinese carps in the Three Gorges Reservoir

3.4.1. Model validation

The one-dimensional hydrodynamic model established by MIKE 11 was verified by fitting the measured and simulated water level data. This study used measured flood processes in July 2010 and July 2012 to calibrate and verify the roughness of the hydrodynamic model respectively based on the measured water level regime at 17 hydrological stations along the reservoir area. The simulated water levels of the model fit well with the measurements, and the water level error ranges of different stations were 0.03–0.64 m during the calibration period, and 0.02–0.38 m during the verification period (Yan et al., 2021). The simulation sequence generated by the periodic stationary autoregressive model of daily flow was evaluated by the moment method. The statistical parameters included the dispersion coefficient C_V, coefficient of skewness C_S, mean $\overline{X}$, root-mean-square deviation S, and level 1 autocorrelation coefficient γ_1. When the statistical parameters of each day meet a certain pass rate, it can be considered that the model calculation is accurate and meet the research needs (Jing et al., 2020). The overall pass rate of C_S is $(N/365) \times 100\%$, where N is the number of qualified days in a year. The accuracy of spawning ground positioning also needed to be verified. Based on the measured flood process (i.e., 2011, 2012, 2014), this research simulated the spatial distribution of spawning grounds in the reservoir area in the corresponding years according to the suitability proportion W of each section along the river. This was then compared with the measured spatial location of the spawning ground to prove the accuracy of the FMCCs reproduction suitability model.

3.4.2. Modelling scheme

The spatial distribution of the spawning grounds of the FMCCs under the condition of 2000 stochastic inflow flood events was then simulated and analyzed based on the verified hydrodynamic model and reproduction suitability model. This analysis was mainly carried out in two parts. First, based on the two conditions during the pre- and post-dam periods, the distribution and changes of the spawning grounds of the FMCCs in the Zhutuo–TGD river section under different current conditions were analyzed. Then, to clarify the impact of different dam scenarios on the spawning behavior of the FMCCs, this study further assumed and calculated the suitability of the FMCCs in the TGR under two of the scenarios: the low-dam and middle-dam scenarios. In this study, the no-dam and high-dam scenarios demote the flow condition of the pre- and post-dam periods, respectively. The TGR is currently in a period of normal operation, which corresponds to the high-dam scenario in the simulation process, and the water level in front of the dam is maintained at 155 m. On 1 May of each year, the flow discharge from the TGR is increased in preparation for flood control; thus the water level in front of the dam drops continuously from a starting level of 155 m to 145 m on 10 June. The middle-dam scenario corresponds to the initial operation period of the TGR. The scheduling mode in this scenario is the same as in the normal operation period, but the water level is lower. In the dry season, the water level in front of the dam gradually drops from 140 m to 135 m. In this hypothetical low-dam scenario in this study, the water level in front of the dam follows the same scheduling mode, dropping from 115 m to 105 m. Thus, the four dam scenarios (no-dam, low-dam, middle-dam, and high-dam) were expressed as the different water levels in front of the TGD (Table 3).

Table 3
The water level in front of the Three Gorges Dam under four dam scenarios.

Dam scenario	Water level fluctuation in front of the dam (m)
No-dam	–
Low-dam	115 ~ 105
Middle-dam	140 ~ 135
High-dam	155 ~ 145

4. Results

4.1. Calibration and verification of the stochastic flood model

In this study, the passing rate of each key parameter of the stochastic simulation sequence was tested. Among these parameters, the relative error between the simulated and measured values of the coefficient of skewness C_S was less than 15%, which is qualified; the pass standard for the remaining statistical parameters is no more than 10%. Table 4 shows the passing rate of the statistical parameters of the main inflow stations in the TGR.

According to the parameter passing rate of each station, the simulated value of the parameter fits well with the measured value. The simulation sequence generated by the periodic stationary autoregressive model of daily flow adequately reflects the hydrological characteristics of the measured sequence.

4.2. Simulation accuracy of the four major Chinese carps' reproduction suitability model

Based on the measured floods during the normal operation of the TGR in the post-dam period (i.e., in 2011, 2012, and 2014), the spatial distribution of the spawning grounds under the measured flood situations was analyzed. The results are presented in Table 5.

Against the three measured floods in 2011, 2012, and 2014, the simulated distribution of the spawning grounds was consistent with the situation reflected in the actual annual survey of the TGR. In 2011, the simulated suitable spawning area for the FMCCs in Banan–Xiakouzhen section accounted for 42.3% of the river section. The measured data from Mu et al. (2014) confirmed that this river section was the main spawning ground for the FMCCs in 2011, consistent with the results of this study (Table 5). In 2012, the Banan–Xiakouzhen section was again the main spawning ground for the FMCCs at 65.4% of the river section, consistent with the location of the spawning grounds identified in field investigations by Mu (2014). In 2014, the suitability proportion W of the Zhutuo–Jiangjin, Jiangjin–Banan, and Fuling–Puzituo river sections aligned with the measured data given in Wang et al. (2015), thereby indicating that the spawning grounds were correctly determined by our model. Therefore, the model of FMCCs reproduction suitability established here can be used to accurately locate the spawning grounds of these fishes in the upper reaches of the Yangtze River.

4.3. Distribution of spawning grounds of the four major Chinese carps during the pre- and post-dam periods

4.3.1. Location of the four major Chinese carps' spawning grounds under stochastic flood conditions

This study examined the reproduction suitability of the FMCCs under pre- and post-dam scenarios. The suitability proportion, W, of different river sections under 2000 stochastic flood events was counted to determine the location of the FMCCs' spawning grounds (Table 6). A comparison of the suitability proportions in the pre- and post-dam periods is shown in Fig. 4.

Table 4
The passing rate of statistical parameters of the main inflow stations in the Three Gorges Reservoir.

Station name	C_V	C_S	$\overline{X}$	S	γ_1
Zhutuo	100%	96%	100%	100%	98%
Beibei	95%	89%	96%	97%	73%
Wulong	100%	92%	100%	100%	90%

Table 5
Suitability proportion of each river section under measured flood conditions during the post-dam period.

Serial number	River section	2011	2012	2014
X1	Zhutuo–Jiangjin	10.7%	0.0%	89.3%
X2	Jiangjin–Banan	2.9%	0.0%	40.0%
X3	Banan–Xiakouzhen	42.3%	65.4%	7.7%
X4	Xiakouzhen–Luoqi	27.8%	16.7%	0.0%
X5	Luoqi–Fuling	8.6%	2.9%	5.7%
X6	Fuling–Puzituo	0.0%	0.0%	74.4%
X7	Puzituo–Zhongxian	0.0%	0.0%	3.7%
X8	Zhongxian–Wanzhou	0.0%	2.4%	28.6%
X9	Wanzhou–Yunyang	0.0%	0.0%	0.0%
X10	Yunyang–Guling	0.0%	0.0%	0.0%
X11	Guling–Fengjie	0.0%	0.0%	0.0%
X12	Fengjie–Wushan	0.0%	0.0%	0.0%
X13	Wushan–Badong	0.0%	0.0%	0.0%
X14	Badong–TGD	0.0%	0.0%	0.0%

The calculations indicated that construction of the TGD has greatly impacted the spawning activities of the FMCCs. The scale and locations of the spawning grounds underwent tremendous change. In Table 6, ΔW is the change in W after dam construction relative to before dam construction. Simulation of the pre-dam scenarios (Table 6) shows that the Zhutuo–TGD river section under natural flow conditions is suitable for spawning by the FMCCs with average values of W ranging from 9.3% to 58.5%. The W values for all river sections (except for Puzituo–Zhongxian and Yunyang–Guling at $<$10%) indicate that the spawning grounds of the FMCCs in the pre-dam period are densely distributed in the upper reaches of the Yangtze River, which is consistent with historical survey results and measured data (Yi et al., 1988). Based on the simulated results, the evaluation accuracy of the FMCCs' reproduction suitability model has been further confirmed.

In the pre-dam period, the FMCCs exhibit some spawning activities in the river between Zhutuo and the TGD. However, since the completion of the TGD, the impact on the water body in the reservoir area has become prominent. The reach downstream from Zhongxian is significantly affected, and the flow conditions in front of the dam are not suitable for the FMCCs to reproduce. The spawning activities of the FMCCs show an upstream shift, and some spawning grounds gradually disappear. In the post-dam period, the reach above Zhongxian contains nine spawning grounds for the FMCCs, in the reservoir area between Zhutuo and Yunyang. Especially, the FMCCs have a higher reproduction suitability proportion in the Zhutuo–Jiangjin section with a length of 60 km and in the Banan–Zhongxian section with a length of 255 km (Table 6).

4.3.2. Impact of dam size on the four major Chinese carps' spawning grounds

To clarify the impact of dam size on the spawning behavior of the FMCCs, this study further assumed and calculated the suitability of the FMCCs in the TGR under two of the dam scenarios: the low-dam and middle-dam scenarios (Table 7). The dam size is related to the water level in front of it, as described in Section 3.4.2 and Table 3. Therefore, a simulation of the dam's size can be obtained by controlling the water level at the front of the dam. According to the different dispatching water levels in front of the dam, the pre-dam situation corresponds to the no-dam scenario and post-dam to the high-dam scenarios (Table 6).

The calculation results of the four dam scenarios are shown in Fig. 5, and the changes of W between the three dam conditions and the no dam conditions are listed in Table 8.

Table 6
Suitability proportion *W* of different river sections during the pre- and post-dam periods.

Serial number	River section	Pre-dam period		Post-dam period		Δ*W*
		The range of *W*	The average of *W*	The range of *W*	The average of *W*	
X1	Zhutuo–Jiangjin	0–100%	58.50%	0–89.3%	14.70%	−43.80%
X2	Jiangjin–Banan	0–94.3%	40.00%	0–85.7%	5.40%	−34.60%
X3	Banan–Xiakouzhen	0–92.3%	53.80%	0–92.3%	34.10%	−19.70%
X4	Xiakouzhen–Luoqi	0–88.9%	41.50%	0–88.9%	35.90%	−5.60%
X5	Luoqi–Fuling	0–97.2%	36.10%	0–97.2%	50.40%	14.30%
X6	Fuling–Puzituo	0–96.3%	21.30%	0–96.3%	37.00%	15.70%
X7	Puzituo–Zhongxian	0–74.9%	9.30%	0–97.4%	18.90%	9.60%
X8	Zhongxian–Wanzhou	0–53.8%	12.90%	0–59.5%	2.90%	−10.00%
X9	Wanzhou–Yunyang	0–44.6%	15.80%	0–33.3%	0.20%	−15.60%
X10	Yunyang–Guling	0–31.7%	9.70%	0.00%	0.00%	−9.70%
X11	Guling–Fengjie	0–34.8%	22.10%	0.00%	0.00%	−22.10%
X12	Fengjie–Wushan	0–29.6%	20.50%	0.00%	0.00%	−20.50%
X13	Wushan–Badong	0–39.5%	22.30%	0–13.6%	0.00%	−22.30%
X14	Badong–TGD	0–30.3%	21.80%	0–13.9%	0.00%	−21.80%

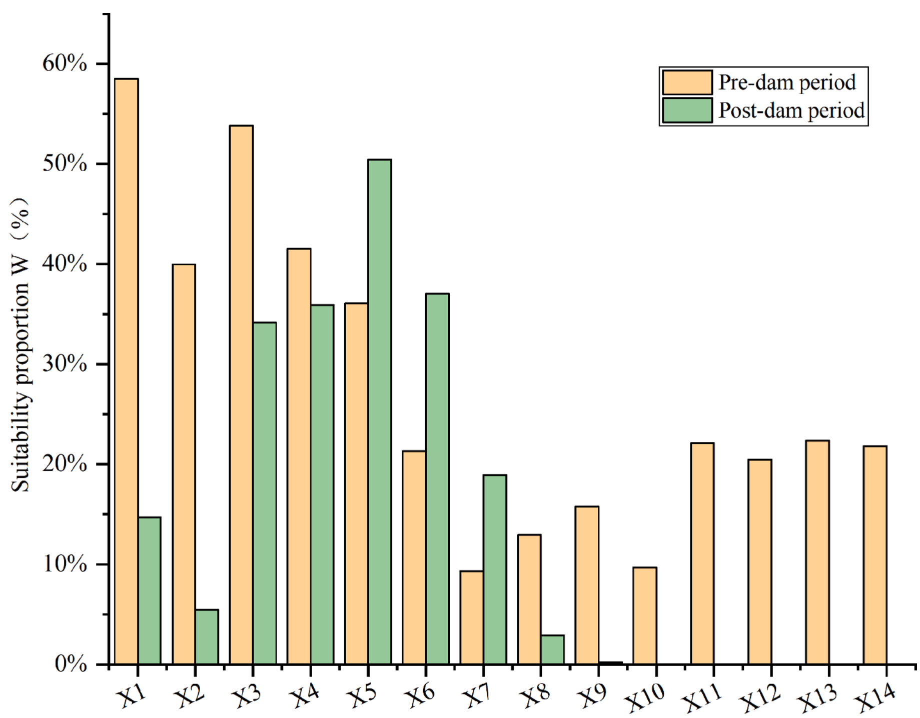

Fig. 4. Distribution of the spawning grounds of the four major Chinese carps in the upper reaches of the Yangtze River in the pre- and post-dam periods.

5. Discussion

Based on the simulation results shown in Table 6, the spawning suitability of FMCCs in the river reaches upstream and downstream of Zhongxian changes with the construction of the TGD. At the head of the TGR, the Zhutuo–Jiangjin and Banan–Zhongxian river sections show relatively high suitability when compared with that in the pre-dam period. A possible explanation is that the high water depth in front of the dam usually changes slowly owning to the influence of backwater, which directly reduces the spawning suitability of the FMCCs in the lower reach of the TGR (Yang et al., 2021). Therefore, the FMCCs have to leave the original river reach to find a more suitable spawning ground in the backwater zone, where the water depth, velocity, water temperature, and water level fluctuation meet the species' spawning requirements (Yang et al., 2021; Yi et al., 2010). The Luoqi–Fuling river section can provide 50.4% of suitable spawning area for the FMCCs, whereas the Puzituo–Zhongxian river section near the middle reaches of the reservoir area can provide 18.9%. The reach above Zhongxian has gradually become a spawning ground for the FMCCs. Although there are cases of proportionally high suitability under certain water flow conditions in the area in front of the dam (e.g., the Wushan–Badong and Badong–TGD river sections can provide 13.6% and 13.9% suitable area during some unusual flood periods, respectively), this area showed a small probability of forming a spawning ground for the FMCCs only during the simulation of multiple floods. Therefore, compared with natural water flows, the impact of dam construction on the spawning grounds of the FMCCs is significant.

Through comparisons of the suitability proportion *W* under the four dam scenarios, the *W* value of each spawning ground in the river section above Zhongxian hardly differs among scenarios in the post-dam period, regardless of the size of the dam (Table 8). The low-dam, middle-dam, and high-dam scenarios correspond to three operational periods of the TGD (i.e., dam water levels of 135 m, 156 m, and 175 m, respectively), which all result in a fluctuating backwater zone of the TGR in the reach above Zhongxian (Gao et al., 2010; Yang et al., 2021). This situation may explain the relatively uniform high suitability proportions in the reach above Zhongxian under the three dam scenarios in the post-dam period. There, the Luoqi–Fuling river section is the most suitable

Table 7
Reproduction suitability of the FMCCs in different river sections under different dam scenarios.

Serial number	River section	Low-dam		Middle-dam	
		The range of *W*	The average of *W*	The range of *W*	The average of *W*
X1	Zhutuo–Jiangjin	0–89.2%	17.2%	0–100%	17.2%
X2	Jiangjin–Banan	0–85.7%	6.7%	0–94.3%	6.8%
X3	Banan–Xiakouzhen	0–92.3%	32.7%	0–92.3%	37.4%
X4	Xiakouzhen–Luoqi	0–88.9%	35.5%	0–88.9%	39.2%
X5	Luoqi–Fuling	0–97.1%	51.6%	0–97.2%	48.7%
X6	Fuling–Puzituo	0–96.3%	41.8%	0–96.3%	39.0%
X7	Puzituo–Zhongxian	0–97.4%	17.9%	0–74.9%	19.5%
X8	Zhongxian–Wanzhou	0–61.9%	11.3%	0–53.8%	3.3%
X9	Wanzhou–Yunyang	0–22.2%	8.1%	0–44.6%	0.2%
X10	Yunyang–Guling	0–17.3%	5.7%	0–31.7%	4.0%
X11	Guling–Fengjie	0–18.7%	9.9%	0–34.8%	5.0%
X12	Fengjie–Wushan	0–20.5%	10.3%	0–29.6%	3.0%
X13	Wushan–Badong	0–22.7%	12.3%	0–39.5%	0.2%
X14	Badong–TGD	0–12.5%	8.1%	0–30.3%	0.2%

spawning ground for the FMCCs. However, significant differences in *W* exist in the sections downstream of Zhongxian under the different dam scenarios. The main reason for this difference could be an increase in the backwater distance caused by the dam construction, which leads to a decrease of velocity and less water level fluctuation in front of the dam. FMCCs cannot get enough flow and velocity stimulation to spawn, so they have to move away from their original spawning grounds and migrate upstream. Under the scenario of building a low dam in the upper reaches of the Yangtze River, the variation trend in values of *W* along the way is consistent with the calculated results of the no-dam scenario, but generally lower than that of the water level without the dam. The sections downstream of Wanzhou will be most affected by the blockage of the dam, at a scale of 64 km. Under the scenario of building the middle and high dams, the river section below Zhongxian is severely affected by the backwater; accordingly, the *W* values are low and suitable spawning grounds gradually disappear from these reaches. Under the middle-dam and high-dam scenarios, 90 km and 101 km of spawning grounds disappear, respectively. Thus, construction of the dam not only directly prevents the downstream FMCCs from returning to spawn, but also causes a decrease in water velocity in front of the dam. The larger size of the dam, the larger influence on the water body in front of the dam, and the slower water level fluctuation. These impacts directly result in a longer backwater distance and a greater loss of spawning grounds with a larger dam. Consequently, the FMCCs gradually migrate upstream after losing suitable spawning conditions. The proportion of suitable spawning ground in the river reach between Luoqi and Zhongxian increases under the three dam sizes, and that in the reach between Zhutuo and Luoqi loses 57 km, 54 km, and 59 km of spawning habitat, under the small, middle, and large-dam scenarios, respectively, accounting for 90%, 60%, and 59% of the total spawning grounds loss. Even though spawning grounds are lost after dam construction, they are mainly distributed in the river reach above Zhongxian, and especially in the Zhutuo-Jiangjin and Banan-Zhongxian river sections.

6. Conclusions

By coupling a hydrodynamic model and a model of FMCCs reproduction suitability, we simulated and analyzed the spatial distribution of spawning grounds of the FMCC, as well as changes in the extent of suitable spawning ground in each river section, in the pre-dam and post-dam periods, in the upper reaches of the Yangtze River under complex inflow conditions. The main conclusions are:

(1) Through the simulation and analysis of the spatial distribution of the spawning grounds of the FMCCs under the stochastic flood process, we determined that locations of suitable spawning grounds shift upstream compared with natural river conditions. In the post-dam period, the FMCCs have a higher reproduction suitability proportion in the Zhutuo–Jiangjin (length 60 km) and Banan–Zhongxian river sections (length 255 km). The reproduction suitability simulations results imply nine suitable spawning grounds for the FMCCs in the upper reaches of the Yangtze River between Zhutuo and Yuyang.

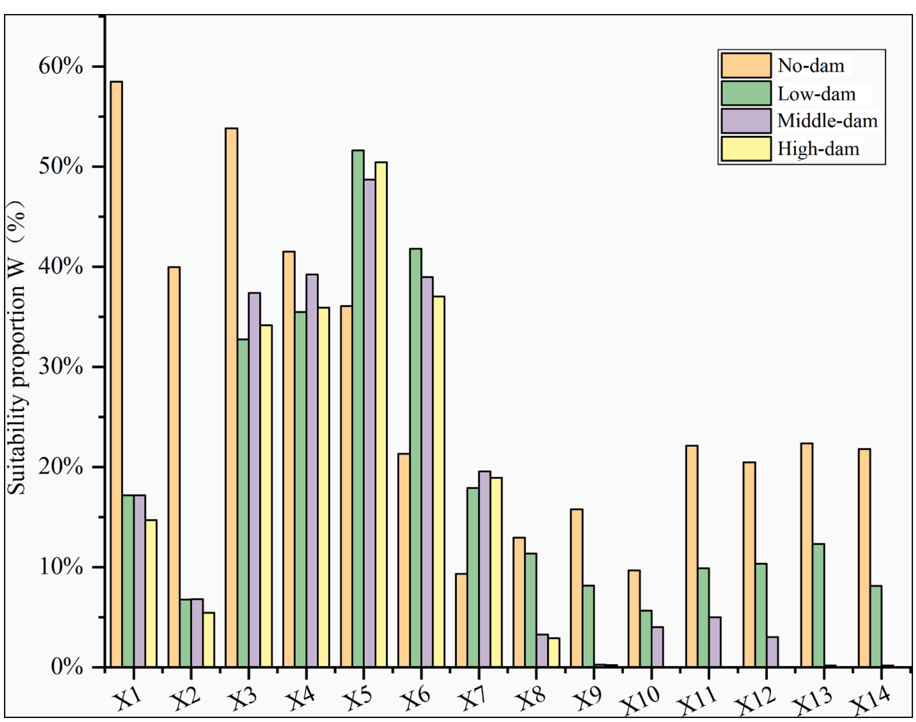

Fig. 5. Distribution of spawning grounds of the four major Chinese carps in the upper reaches of the Yangtze River under the four different dam scenarios.

Table 8
Changes in reproduction suitability of four major Chinese carps in the Three Gorges Reservoir under different dam sizes compared with the no-dam scenario.

Serial number	River section	*W* of the pre-dam period	△*W*			Net loss of spawning grounds (km)		
			Low-dam	Middle-dam	High-dam	Low-dam	Middle-dam	High-dam
X1	Zhutuo–Jiangjin	58.50%	−41.30%	−41.30%	−43.80%	24.78	24.78	26.28
X2	Jiangjin–Banan	40.00%	−33.30%	−33.20%	−34.60%	23.64	23.57	24.57
X3	Banan–Xiakouzhen	53.80%	−21.10%	−16.40%	−19.70%	5.91	4.59	5.52
X4	Xiakouzhen–Luoqi	41.50%	−6.00%	−2.30%	−5.60%	3.12	1.20	2.91
X5	Luoqi–Fuling	36.10%	15.50%	12.60%	14.30%	−9.77	−7.94	−9.01
X6	Fuling–Puzituo	21.30%	20.50%	17.70%	15.70%	−8.41	−7.26	−6.44
X7	Puzituo–Zhongxian	9.30%	8.60%	10.20%	9.60%	−6.11	−7.24	−6.82
X8	Zhongxian–Wanzhou	12.90%	−1.60%	−9.60%	−10.00%	1.26	7.58	7.90
X9	Wanzhou–Yunyang	15.80%	−7.70%	−15.60%	−15.60%	4.16	8.42	8.42
X10	Yunyang–Guling	9.70%	−4.00%	−5.70%	−9.70%	1.32	1.88	3.20
X11	Guling–Fengjie	22.10%	−12.20%	−17.10%	−22.10%	4.64	6.50	8.40
X12	Fengjie–Wushan	20.50%	−10.20%	−17.50%	−20.50%	4.28	7.35	8.61
X13	Wushan–Badong	22.30%	−10.00%	−22.10%	−22.30%	5.40	11.93	12.04
X14	Badong–TGD	21.80%	−13.70%	−21.60%	−21.80%	9.59	15.12	15.26

Note: The negative value denoting a net loss of spawning ground represents a greater river reach length as compared with in the pre-dam period.

(2) Through the simulation of four dam scenarios in the TGR in comparison with pre-dam river conditions, construction of the dam leads to FMCCs' spawning ground losses of 64 km under the low-dam scenario, 90 km under the middle-dam scenario, and 101 km under the high-dam scenario. The spawning ground lost in the reach between Zhutuo and Luoqi accounts for 90%, 60%, and 59% of the total net loss, respectively, under the three dam sizes. These results show that the ecological suitability of a dammed river for aquatic organisms is affected to varying degrees depending on the size of the dam.

CRediT authorship contribution statement

Caihong Tang: Methodology, Writing – review & editing. **Qiming Yan:** Methodology, Writing – original draft. **Wenda Li:** Validation. **Xiyan Yang:** Data curation. **Shanghong Zhang:** Conceptualization, Funding acquisition, Writing – review & editing.

Declaration of Competing Interest

The authors declare that they have no known competing financial interests or personal relationships that could have appeared to influence the work reported in this paper.

Acknowledgments

This study was supported by the National Natural Science Foundation of China (52061135104). We thank Dr. Natalie Kim from Liwen Bianji, Edanz Editing China (www.liwenbianji.cn/ac), for editing the English text of a draft of this manuscript.

References

Ban, X., Diplas, P., Shih, W., Pan, B., Xiao, F., Yun, D., 2019. Impact of Three Gorges Dam operation on the spawning success of four major Chinese carps. Ecol. Eng. 127, 268–275.
Brown, S.K., Buja, K.R., Jury, S.H., Monaco, M.E., Banner, A., 2000. Habitat suitability index models for eight fish and invertebrate species in Casco and Sheepscot Bays, Maine. North Am. J. Fish. Manag. 20 (2), 408–435.
Cao, W.X., Yu, Z.T., Xu, Y.X., 1987. In: Preliminary evaluation of the impact of the Three Gorges Project on Minjiang fish resources and research on the ways of resource proliferation. Collection of Research Papers on the Impact of the Three Gorges Project on the Ecology and Environment. Science Press, Beijing, p. 318 [in Chinese].
Chen, J., Li, Q.Q., 2015. Assessment of eco-operation effect of Three Gorges Reservoir During trial run period. J. Yangtze River Sci. Res. Inst. 32 (4), 1–6 [in Chinese].
Cho, Y., Lee, W.C., Hong, S., Kim, H.C., Kim, J.B., 2012. GIS-based suitable site selection using habitat suitability index for oyster farms in Geoje-Hansan Bay, Korea. Ocean Coast. Manag. 56, 10–16.
Corbacho, C., Sanchez, J.M., 2001. Patterns of species richness and introduced species in native freshwater fish faunas of a Mediterranean-type basin: the Guadiana River (southwest Iberian Peninsula). Regulated Rivers: Res. Manage.: Int. J. Devoted River Res. Manage. 17 (6), 699–707.
Galat, D.L., Lipkin, R., 2000. Restoring ecological integrity of great rivers: historical hydrographs aid in defining reference conditions for the Missouri River. In: Jungwirth, M., Muhar, S., Schmutz, S. (Eds.), Assessing the Ecological Integrity of Running Waters. Springer Netherlands, Dordrecht, pp. 29–48.
Gao, X., Zeng, Y., Wang, J.W., Liu, H.Z., 2010. Immediate impacts of the second impoundment on fish communities in the Three Gorges Reservoir. Environ. Biol. Fishes 87, 163–173.
Garcia, T., Murphy, E.A., Jackson, P.R., Garcia, M.H., 2015. Application of the FluEgg model to predict transport of Asian carp eggs in the Saint Joseph River (Great Lakes tributary). J. Great Lakes Res. 41 (2), 374–386.
Gharari, S., Razavi, S., 2018. A review and synthesis of hysteresis in hydrology and hydrological modeling: Memory, path-dependency, or missing physics? J. Hydrol. 566, 500–519.
Ban, X., Li, D.M., Li, D., 2009. Application of habitat suitability criteria on spawn-sites of Chinese sturgeon in downstream of Gezhouba Dam. Eng. J. Wuhan Univ. 42 (2), 172−177 (in Chinese).
Jiang, N., Jiang, B., Lei, G.P., 2019. Influence of waterway regulation project on habitat suitability index of Four Major Chinese Carps in Dongliu channel in lower Yangtze River. Yangtze River 50(05), 5−9. [in Chinese].
Jiang, W., Liu, H.Z., Duan, Z.H., Cao, W.X., 2010. Seasonal variation in drifting eggs and larvae in the Upper Yangtze, China. Zool. Sci. 27 (5), 402–409.
Jing, Z., An, W.J., Zhang, S.H., Xia, Z.X., 2020. Flood control ability of river-type reservoirs using stochastic flood simulation and dynamic capacity flood regulation. J. Clean. Prod. 257, 120809.
Knudson, M.D., VanLooy, J.A., Hill, M.J., 2015. A habitat suitability index (HSI) for the Western Prairie Fringed Orchid (*Platanthera praeclara*) on the Sheyenne National Grassland, North Dakota, USA. Ecol. Ind. 57, 536–545.
Li, C., Liao, W.G., Chen, D.Q., Xu, T.B., Liu, S.P., Liu, J.H., 2008. Hydrodynamic effect of different regulation scenarios for Three Gorges Reservoir on Four Major Chinese Carps spawning. Sci. Technol. Rev. 26 (17), 55–61.
Li, S., Lu, J.Y., Cheng, Z.H., Lu, B.H., Hou, P., 2018. Ecological runoff and its ecological operation of Three Gorges Reservoir. Water Power 44 (06), 7–12 [in Chinese].
Li, M.Z., Ma, Q., Chen, L., Liu, H.Z., 2020. Natural reproduction and hydrologic requirements of pelagophil fish in the Three Gorges Reservoir. Acta Hydrobiol. Sin. 1–13 [in Chinese].
Liu, M., Lin, J., Peng, Q., Yu, L., Chen, D., Liu, S., Duan, X., 2018. Relationship between the distribution of broodstock and vorticity of spawning grounds of Four Major Chinese Carps in the Middle Reaches of the Yangtze River during ecological operation of the Three Gorges Dam. Water 10 (10), 1487.
Lytle, D.A., Poff, N.L., 2004. Adaptation to natural flow regimes. Trends Ecol. Evol. 19 (2), 94–100.
MacDougall, T.M., Wilson, C.C., Richardson, L.M., Lavender, M., Ryan, P.A., 2007. Walleye in the Grand River, Ontario: an overview of rehabilitation efforts, their effectiveness, and implications for eastern Lake Erie fisheries. J. Great Lakes Res. 33 (sp1), 103–117.
Morita, K., Yamamoto, S., 2002. Effects of habitat fragmentation by damming on the persistence of stream-dwelling charr populations. Conserv. Biol. 16 (5), 1318–1323.
Mu, H.X., 2014. Study on early fish resource ecology in the end section of the Three Gorges Reservoir and in front of the Three Gorges Dam. Institute of Hydrobiology, Chinese Academy of Science [in Chinese].
Mu, H., Li, M., Liu, H., Cao, W., 2014. Analysis of fish eggs and larvae flowing into the Three Gorges Reservoir on the Yangtze River, China. Fish. Sci. 80 (3), 505–515.
Prada, A.F., George, A.E., Stahlschmidt, B.H., Chapman, D.C., Tinoco, R.O., Mendoza-Lera, C., 2018. Survival and drifting patterns of grass carp eggs and larvae in response to interactions with flow and sediment in a laboratory flume. PLoS ONE 13 (12), e0208326.
Ren, S., Zhang, B., Wang, W.-J., Yuan, Y., Guo, C., 2021. Sedimentation and its response to management strategies of the Three Gorges Reservoir, Yangtze River, China. CATENA 199, 105096.

Santos, J.M., Ferreira, M.T., Pinheiro, A.N., Bochechas, J.H., 2006. Effects of small hydropower plants on fish assemblages in medium-sized streams in central and northern Portugal. Aquat. Conserv. Mar. Freshwater Ecosyst. 16 (4), 373–388.

Wang, Y.K., Zhang, N., Wang, D., Wu, J.C., 2020. Impacts of cascade reservoirs on Yangtze River water temperature: Assessment and ecological implications. J. Hydrol. 590, 125240.

Wang, Y., Gao, Q.H., 2017. Correlation analysis on hydrological processes and spawning behavior of Four Major Chinese Carps. Yangtze River 48 (06), 24–27 [in Chinese].

Wang, J., Li, C., Duan, X., Chen, D., Feng, S., Luo, H., Peng, Q., Liao, W., 2014a. Variation in the significant environmental factors affecting larval abundance of four major Chinese carp species: fish spawning response to the Three Gorges Dam. Freshw. Biol. 59 (7), 1343–1360.

Wang, J.N., Li, C., Duan, X.B., Luo, H.H., Feng, S.X., Peng, Q.D., Liao, W.G., 2014b. The relationship between thermal regime alteration and spawning delay of the four major Chinese carps in the Yangtze River below the Three Gorges Dam. River Res. Appl. 30 (8), 987–1001.

Wang, H.L., Li, M.Z., Gao, X., Liu, H.Z., Cao, W.X., 2015. The status of the early stage fish resources in the Fengdu section of the Three Gorges Reservoir. Acta Hydrobiol. Sin. 39 (05), 954–964 [in Chinese].

Wang, S.Y., Liao, W.G., Chen, D.Q., Duan, X.B., Peng, Q.D., Wang, K., Li, C., 2008. Analysis of Eco-Hydrological characteristics of the four Chinese farmed Carps' spawning grounds in the middle reach of the Yangtze River. Resour. Environ. Yangtze Basin 17 (06), 892–897 [in Chinese].

Yan, Q.M., Jing, Z., Xia, Z.X., Zhang, S.H., 2021. Flood control capacity of the Three Gorges Project for different frequency floods. Environ. Eng. Sci. 2021 (38), 1195–1205.

Yang, S.F., Xu, G.B., Wang, L., Yang, W., Xiao, Y., Li, W.J., Hu, J., 2021. Field-derived relationships between fish habitat distribution and flow-sediment conditions in fluctuating backwater zone of the Three Gorges Reservoir. Ecol. Inform. 62, 101273.

Yang, Z., Gong, Y., Dong, C., Qiao, Y., Chen, X.J., Tang, H.Y., 2017. Temporal and spatial distribution of the four major Chinese carp species in Three Gorges Reservoir during the normal operating period. J. Hydroecol. 38 (05), 72–79 [in Chinese].

Yi, Y.J., Le, S.H., 2011. Habitat suitability function of four major Chinese Carps spawning sites in the Yangtze River. J. Basic Sci. Eng. 19, 117–122 [in Chinese].

Yi, Y., Wang, Z., Yang, Z., 2010. Impact of the Gezhouba and Three Gorges Dams on habitat suitability of carps in the Yangtze River. J. Hydrol. 387 (3-4), 283–291.

Yi, B.L., Yu, Z.T., Liang, Z.S., 1988. Gezhouba water control project and four famous fishes in Yangtze River. Hubei Science and Technology Press, Wuhan, pp. 1–46 [in Chinese].

Yu, M., Yang, D., Liu, X., Li, Q., Wang, G., 2019. Potential impact of a large-size cascade reservoir on the spawning conditions of critical species in the Yangtze River, China. Water 11 (10), 2027.

Zhang, S.H., Jing, Z., Yi, Y.J., Wu, Y., Zhao, Y., 2017. The dynamic capacity calculation method and the flood control ability of the Three Gorges Reservoir. J. Hydrol. 555, 361–370.